

5128-89

N93-19241-4 549

INTERPRETING ASTEROID PHOTOMETRY AND POLARIMETRY USING  
 A MODEL OF SHADOWING AND COHERENT BACKSCATTERING

Yu. G. Shkuratov † and K. Muinonen ‡

† Astronomical Observatory of Kharkov State Univ., Sumskaya Street 35, Kharkov 310022, Ukraine  
 ‡ Lowell Observatory, 1400 West Mars Hill Road, Flagstaff, AZ 86001, U.S.A.

The shadow-hiding models for the opposition effect (Hapke 1966, Lumme and Bowell 1981) and negative polarization (Wolff 1975) of atmosphereless solar system bodies do not explain some experimental findings, such as the enhancing opposition effect and negative polarization with decreasing particle size down to wavelength scales. Figure 1 shows the enhancement for laboratory photometric and polarimetric data on artificial glass samples with different particle size (Shkuratov 1985, Shkuratov and Akimov 1987). These results are in agreement with the so-called coherent backscattering or interference mechanism proposed for the interpretation of the opposition effect and negative polarization by Shkuratov (1985) and Muinonen (1989).

We have developed two different approaches for describing the opposition effect and negative polarization produced by the shadow-interference mechanism. One is based on exact electromagnetic solutions for simple scattering systems that include dipole-dipole and dipole-surface coupling; surface-surface coupling was studied in the geometric optics approximation (Muinonen 1989 and 1990ab, Muinonen *et al.* 1990, Muinonen and Lumme 1991). The other is based on a point-scatterer approximation characterized by model photometric and polarimetric phase functions, and the mutual shadowing effect is derived using virtual volumes associated with the point-scatterers (Shkuratov 1988 and 1991, Shkuratov *et al.* 1989). Both approaches yield qualitatively similar results, although neither is entirely satisfactory. We regard them as prototypes for a future unified model of shadowing and coherent backscattering. The sharp opposition effect of 44 Nysa and the asteroid albedo-polarization rule are here explained using the point-scatterer approach. (FNU)

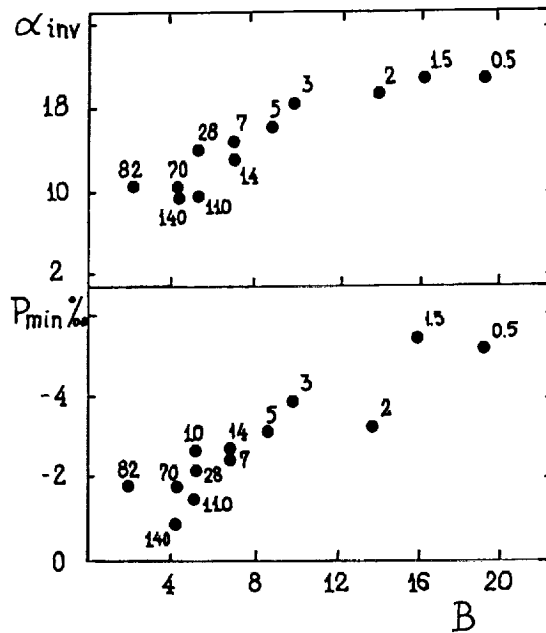


Fig. 1. Inversion phase angle  $\alpha_{inv}$  and minimum  $P_{min}$  of linear polarization for artificial glass powders versus the opposition effect curvature  $B = 10^3 \times [A(1^\circ/5) + A(12^\circ/5) - 2A(7^\circ)] / 5^\circ/5$ , where  $A$  is the bidirectional reflectance. Particle size is shown in microns for each data point.

OPPOSITION EFFECT OF 44 NYSA

Including the mutual shadowing and coherent backscattering effects but presently excluding rough surface shadowing, we describe the bidirectional reflectance by

$$A(\iota, \epsilon, \alpha) = \frac{\varpi \cos \iota \cos \epsilon}{4 \cos \iota + \cos \epsilon} [\chi(\alpha)T(\iota, \epsilon, \alpha) + D(\iota, \epsilon, \alpha)M(\iota, \epsilon, \alpha)], \tag{1}$$

where  $\varpi$  is the average single particle albedo,  $\iota$  and  $\epsilon$  are the angles of incidence and emergence, and  $\alpha$  is the phase angle. Also,  $\chi$  is the average single particle phase function, and  $T$ ,  $D$ , and  $M$  are the mutual shadowing, coherent backscattering, and multiple scattering functions, respectively. Assuming an isotropic single-particle phase function, we obtain (Shkuratov *et al.* 1991)

$$T(\iota, \epsilon, \alpha) = \sum_{n=0}^{\infty} \frac{(\cos \iota + \cos \epsilon)^{n+1}}{2^n \prod_{m=0}^n (\cos \iota + \cos \epsilon + mq \sin \alpha)}, \quad q = \frac{\xi}{1 - \xi}$$

$$M(\iota, \epsilon, \alpha) = \left( \frac{1 + 2 \cos \iota}{1 + 2 \cos \iota \sqrt{1 - \varpi}} \right) \left( \frac{1 + 2 \cos \epsilon}{1 + 2 \cos \epsilon \sqrt{1 - \varpi}} \right) - 1 \tag{2}$$

$$D(\iota, \epsilon, \alpha) = 1 + \frac{1}{\sqrt{1 + L^2[\sin^2 \iota + \sin^2 \epsilon + 2(\cos \iota \cos \epsilon - \cos \alpha)]}}, \quad L = \frac{4\pi r}{\lambda}(1 + \varpi) \sqrt{\frac{\varpi}{3(1 - \varpi)}}$$

where  $\xi$  is the volume density of the scattering medium and  $L$  is the average size of a ‘flare spot’ caused by multiple scattering within the surface.  $\lambda$  and  $r$  are the wavelength and the average particle radius. The present scattering model gives an enhancement of the opposition effect with increasing albedo due to the multiple scattering term  $D(\iota, \epsilon, \alpha)M(\iota, \epsilon, \alpha)$ . In Figure 2, this is illustrated for model parameters  $\xi = 0.5$ ,  $r/\lambda = 1$ ,  $\varpi = 0.5$  (curve 1) and  $\varpi = 0.85$  (curve 2), assuming that  $\iota = 0^\circ$  and  $\epsilon = \alpha$ . Also, a slight wavelength dependence is predicted for the opposition effect in the case of spectrally neutral particulate media, illustrated by the ratio  $A(\alpha; r/\lambda = 1.2)/A(\alpha; r/\lambda = 0.8)$  (curve 3).

Besides theoretical results, Figure 2 shows the observations by Harris *et al.* (1989) for the bright E-class asteroid 44 Nysa with geometric albedo about 45%. We emphasize that the asteroid data are disk-integrated, whereas the theoretical scattering law is for a local surface element. Thus, we treat 44 Nysa as if it were a planar disk, the normal of which points in the direction of the Sun. For small phase angles and for the present demonstration purposes, this simple assumption is justified. The observations are explained by the coherent backscattering mechanism without introducing unrealistically small volume densities.

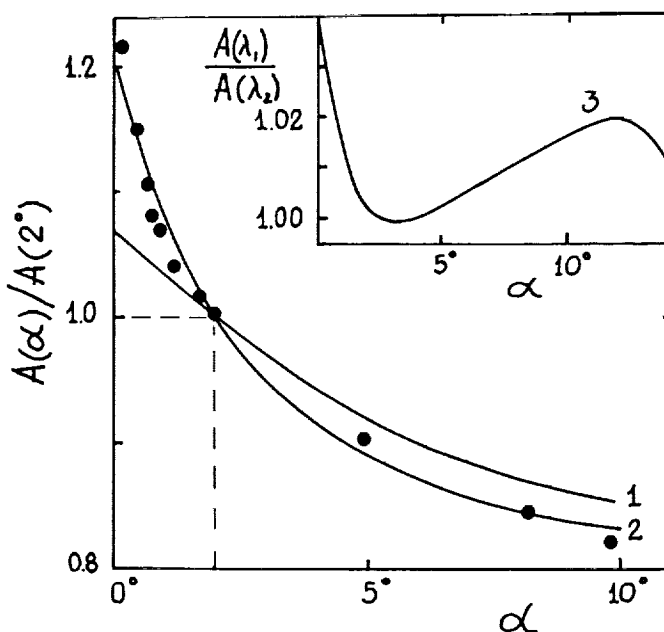


Fig. 2. Opposition effect dependence on single particle albedo (curves 1, 2), and on wavelength (curve 3). Observations by Harris *et al.* (1989) for 44 Nysa are explained by the coherent backscattering mechanism.

## ALBEDO-POLARIZATION LAW

An approximate expression for the degree of linear polarization has been obtained by assuming an isotropic scattering phase function and a modified Rayleigh polarization  $G \sin^2 \alpha / (1 + \cos^2 \alpha)$  (scale factor  $0 < G \leq 1$ ) for single particles (Shkuratov 1991, Shkuratov and Melkumova 1991),

$$P(\alpha) = \frac{G}{18} (1 + 2\sqrt{1 - \varpi})^2 \left\{ \sin^2 \alpha + \frac{2\xi \varpi [1 - \sqrt{1 + \varrho^2 \sin^2 \alpha}]^2}{\varrho^2 \sin^2 \alpha \sqrt{1 + \varrho^2 \sin^2 \alpha} \ln(1 - \xi)} \right\}, \quad \varrho = \frac{8\pi r}{3\lambda \ln(1 - \xi)}. \quad (3)$$

We will now study the correlation of asteroid geometric albedos and polarization curves. The geometric albedos of dark asteroids, derived from thermal radiometry and polarimetry, differ from each other, as has been long known (Morrison 1977, Zellner *et al.* 1977). This difference occurs at low albedos in the dependence  $\log p + k \log h = b$ , where  $p$  is the geometric albedo,  $h$  is the polarization slope, and  $k$  and  $b$  are constants. No convincing explanation has been offered for this. Figure 3 shows our model dependencies  $\log A(\alpha = 5^\circ) + k \log h = b$  for the parameters  $r/\lambda = 0.5$ ,  $\xi = 0.4$ , and  $G = 0.2$  (curve 1),  $G = 0.9$  (curve 2). Thus, our albedo is the reflectance at the  $5^\circ$  phase angle, and this definition is used for both experimental and theoretical results. The filled circles present terrestrial samples (Zellner *et al.* 1977), and crosses are experimental data for mixtures of magnesium oxide and soot (Shkuratov and Akimov 1987). Laboratory measurements for mixtures of water-color pigments are also shown (dashed line).

Shkuratov (1980) attempted to interpret the experimentally verified saturation; using the present models this interpretation can be significantly improved. The theoretical curves consist of three major parts. The first high-albedo part, i.e. albedos larger than 10%, is approximately linear, undoubtedly according to the so-called Umov law. The second part, in the albedo range of 2–7%, results from a small contribution of multiple scattering. In the third part, for albedos smaller than 2%, the polarization slope flattens again: this derives from the decreasing amount of second-order scattering causing the negative polarization.

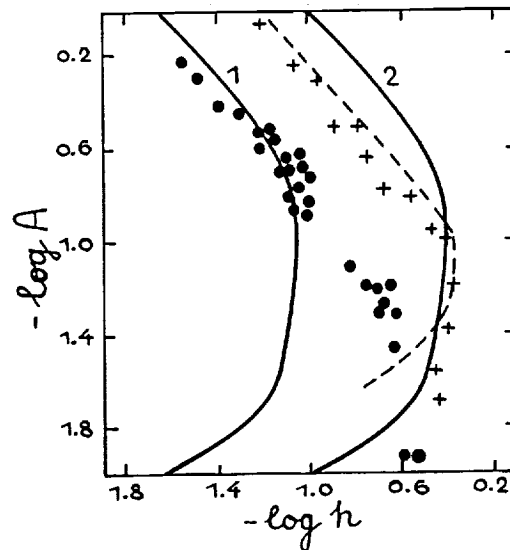


Fig. 3. Experimental and theoretical relations between albedo  $A(\alpha = 5^\circ)$  and polarization slope  $h$ .

## CONCLUSION

Three particular results for asteroids can be stated:

- The observed opposition effect and negative polarization require the existence of micron-scale fine structure in regolith particles. Although such small-scale structure has been widely assumed in the past, it is not predicted by previous theoretical models.

- A sharp and narrow opposition effect (the opposition spike) has recently been observed for some bright asteroids. In contrast, weak or non-existent opposition effects are exhibited by some dark asteroids. Such observations are explained by the coherent backscattering mechanism.
- The difference in radiometric and polarimetric albedos of dark asteroids is caused by the non-linearity of the relationship between geometric albedo and polarization slope.

## References

- Hapke B. (1966) An improved lunar theoretical phase function. *Astron. J.*, **71**, 5, 333-339.
- Harris A. W., Young I. W., Contreiras L., Dockweiler T., Belkora L., Salo H., Harris W. D., Bowell E., Poutanen M., Binzel R. P., Tholen D. I., and Wang S. (1989) Phase relations of high-albedo asteroids: the unusual opposition brightening of 44 Nysa and 64 Angelina. *Icarus*, **81**, 356-374.
- Lumme K. and Bowell E. (1981) Radiative transfer in the surfaces of atmosphereless bodies. I. Theory. *Astron. J.*, **86**, 11, 1694-1704.
- Morrison D. (1977) Asteroid sizes and albedos. *Icarus*, **31**, 185-220.
- Muinonen K. (1989) Electromagnetic scattering by two interacting dipoles. Proc. 1989 URSI EM-Theory Symp. (Stockholm), 428-430.
- Muinonen K. (1990a) Ph.D. thesis, University of Helsinki.
- Muinonen K. (1990b) Scattering of light by solar system dust: the coherent backscatter phenomenon. 1990 Proc. Finnish Astron. Soc., 12-15.
- Muinonen K., Sihvola A. H., Lindell I. V., and Lumme K. (1991) Scattering by a small object close to an interface. II. Study of backscattering. *J. Opt. Soc. Am. A*, **8**, 477-482.
- Muinonen K. and Lumme K. (1991) Light scattering by solar system dust: the opposition effect and the reversal of linear polarization. In *IAU Colloquium 126, Origin and Evolution of Dust in the Solar System*, 159-162. Kluwer Academic Press.
- Shkuratov Yu. G. (1980) Albedo of asteroids. *Sov. Astron. J.*, **57**, 6, 1320-1322.
- Shkuratov Yu. G. (1985) On opposition brightness surge and light negative polarization of solid cosmic surfaces. *Astron. Circ.*, **1400**, 3-6.
- Shkuratov Yu. G. (1988) Diffractional model of the brightness surge of light scattered by solid surface of celestial bodies. *Kin. Phys. Neb. Tel.*, **4**, 4, 33-39.
- Shkuratov Yu. G. (1991) Interference model of the negative polarization of light scattered by solid surface of celestial bodies. *Sov. Astron. Vestn.*, **25**, 2, 152-161.
- Shkuratov Yu. G. and Akimov L. A. (1987) Laboratory studies of negative polarization of light scattered by complex structure surfaces. Some consequences for atmosphereless cosmic bodies. I. *Kin. Phys. Neb. Tel.*, **3**, 2, 22-27.
- Shkuratov Yu. G. and Melkumova L. Ya. (1991) Diffractional model of the negative polarization of light scattered by atmosphereless cosmic bodies. Lunar and Planet. Sci. Conf. XXII, 1243-1244.
- Shkuratov Yu. G., Opanasenko N. V., and Melkunova L. Ya. (1989) Interference surge of backscattering and negative polarization of light reflected by complex structure surfaces. Preprint 361, IRE AS USSR, 1-26.
- Shkuratov Yu. G., Opanasenko N. V., Basilevsky A. T., Zhukov B. S., Kreslavsky M. A., and Murchie S. (1991) A possible interpretation of bright features on the surface of Phobos. *Planet. Space Sci.*, **39**, 1/2, 341-347.
- Wolff M. (1975) The polarization of light reflected by rough planetary surface. *Appl. Opt.*, **14**, 6, 1395-1404.
- Zellner B., Leake M., Leberte T., Duseaux M., and Dollfus A. (1977) The asteroid albedo scale. I. Laboratory polarimetry of meteorites. Proc. 8th Lunar Sci. Conf., 1091-1110.